LA-UR-21-20831 (Accepted Manuscript)

Structural and Spectroscopic Comparison of Soft-Se vs. Hard-O Donor Bonding in Trivalent Americium/Neodymium Molecules

Goodwin, Conrad Alexander Phillip; Schlimgen, Anthony William; Albrecht-Schönzart, Thomas E; Batista, Enrique Ricardo; Gaunt, Andrew James; Janicke, Michael Timothy; Kozimor, Stosh Anthony; Scott, Brian Lindley; Stevens, Lauren Marie; White, Frankie Don Jr.; Yang, Ping

To be published in: Angewandte Chemie International Edition

DOI to publisher's version: 10.1002/anie.202017186

Permalink to record: http://permalink.lanl.gov/object/view?what=info:lanl-repo/lareport/LA-UR-21-20831

Structural and Spectroscopic Comparison of Soft-Se vs. Hard-O Donor Bonding in Trivalent Americium/Neodymium Molecules

Conrad A. P. Goodwin[+], Anthony W. Schlimgen[+], Thomas E. Albrecht-Schönzart, Enrique R. Batista, Andrew J. Gaunt,* Michael T. Janicke, Stosh A. Kozimor, Brian L. Scott, Lauren M. Stevens, Frankie D. White, and Ping Yang**

Abstract: *Covalency is often considered to be an influential factor in driving An^{3+} vs. Ln^{3+} selectivity invoked by soft donor ligands. This is intensely debated, particularly the extent to which An^{3+}/Ln^{3+} covalency differences prevail and manifest as the f-block is traversed, and the effects of periodic breaks beyond Pu. Herein, two Am complexes, $[Am\{N(E{=}PPh_2)_2\}_3]$ (**1-Am**, E = Se; **2-Am**, E = O) are compared to isoradial $[Nd\{N(E{=}PPh_2)_2\}_3]$ (**1-Nd**, **2-Nd**) complexes. Covalent contributions are assessed and compared to U/La and Pu/Ce analogues. Through ab initio calculations grounded in UV-vis-NIR spectroscopy and single-crystal X-ray structures, we observe differences in f orbital involvement between Am–Se and Nd–Se bonds, which are not present in O-donor congeners.*

Introduction

The minor actinides, Am and Cm, are significant contributors to the long-term radiological burden of used nuclear fuel, leading to proposals for their separation and transmutation into less hazardous isotopes.[1] However, the trivalent oxidation state dominates the chemistry of Am and Cm and also the lanthanide (Ln) fission products; therefore, separation based on redox chemistry is difficult.[2] Historically, both An^{3+} and Ln^{3+} ions have been considered to engage in largely ionic bonding modes with a wide array of ligands, exhibiting very similar chemical behavior that renders An^{3+}/Ln^{3+} separation a significant challenge. Differences in the bonding between Am^{3+} ions and soft donor ligands vs. analogous Ln^{3+} ions have been exploited to affect selectivity at laboratory-scale,[3] but currently, practical limitations exist regarding process-scale implementation.[4]

Early actinides (Th-Pu) have energetically accessible 5f orbitals as well as 6d and 7p orbitals which have larger radial extensions and are often significantly involved in bonding. This allows Th-/U-ligand bonding to be partially covalent due to overlap of ligand and metal orbitals.[5] For the early actinides, differential covalency can manifest structurally as shorter metal–ligand bonds (compared to lanthanide congeners) with various soft donors such as nitrogen heterocycles and thioethers, as determined by X-ray diffraction techniques.[3a,6] These effects can become small for Am[7] where more sensitive spectroscopic techniques are required to observe bonding differences to these light atoms.[8] By the middle of the An series (Am-Cf) there is a significant contraction of the 5f orbitals, and concomitant lowering of their energy. Here, there is poor 5f orbital overlap but, depending on the ligand, there can be favorable energy matching between ligand and metal valence orbitals: this can lead to energy degeneracy-driven covalency.[5,9] The two mechanisms of overlap-driven and energy-degeneracy-driven covalency are significant for different parts of the An series, and complicate comparisons of early and middle An elements.[9c,d,10] Topological methods, such as the quantum theory of atoms in molecules (QTAIM), describe Am-Cf as predominantly ionic in their bonding, in accord with conventional thought,[9d,10b,11] while recent experimental approaches have focused on measuring physical manifestations of electronic structure differences.[5b,12]

The comparison of multiple donor-atom systems on a metal ion across homologous molecular series provides a systematic approach capable of teasing out subtle bonding and electronic structure periodic trends in a more convincing manner than standalone studies of a single metal or donor type; such experimental studies are extremely rare for transuranium elements.[13] Some of us have previously reported *tris*-imidodiphosphinochalcogenide, $[M\{N(E{=}PR_2)_2\}_3]$, complexes for U/Pu, and their isoradial Ln congeners La/Ce, where E = S (R = *i*Pr, Ph), Se (R = *i*Pr, Ph), Te (R = *i*Pr) and M = metal.[13] Analysis of M-E bond lengths in conjunction with density functional theory (DFT) and QTAIM computational analysis allowed a clear conclusion to be drawn that the data was consistent with an enhancement of covalency in An–E vs. Ln–E bonding. Attempting to

[*] C. A. P. Goodwin,[+] A. J. Gaunt, M. T. Janicke, S. A. Kozimor, L. M. Stevens, F. D. White
Chemistry Division, Los Alamos National Laboratory
Los Alamos, NM 87545 (USA)
E-mail: gaunt@lanl.gov
A. W. Schlimgen,[+] E. R. Batista, P. Yang
Theoretical Division, Los Alamos National Laboratory
Los Alamos, NM 87545 (USA)
E-mail: erb@lanl.gov
pyang@lanl.gov
T. E. Albrecht-Schönzart
Department of Chemistry and Biochemistry, Florida State University
95 Chieftain Way, Tallahassee, FL 32306 (USA)
B. L. Scott
Materials Physics and Applications Division
Los Alamos National Laboratory
Los Alamos, NM 87545 (USA)
[+] These authors contributed equally to this work.
Supporting information and the ORCID identification number(s) for the author(s) of this article can be found under: https://doi.org/10.1002/anie.202017186.

understand more subtle Am/Ln differences in a comparable study has been impeded by a lack of well-developed Am synthetic chemistry methods along with radiological and isotope availability considerations. Recent advances in air-/moisture-free Am chemistry now permit us to compare hard O- and soft Se-donor complexes,[12d,14] $[Am\{N(E{=}PPh_2)_2\}_3]$ (E = Se, **1-Am**; O, **2-Am**), to their isoradial Nd congeners $[Nd\{N(E{=}PPh_2)_2\}_3]$ (**1-Nd**, **2-Nd**). We have examined the bonding and electronic structure in these complexes by single crystal X-ray diffraction, UV-vis-NIR spectroscopy, multinuclear NMR spectroscopy, and ab initio calculations.

Results and Discussion

^{243}Am is a scarce resource. Each reaction was pre-optimized with a goal of yielding X-ray quality single crystals on the first attempt. The rationale for selecting the LSe, $\{N(Se{=}PPh_2)_2\}^{1-}$, ligand to prepare **1-Am** and **1-Nd** was that previous studies comparing U^{3+}/La^{3+} and Pu^{3+}/Ce^{3+} pairs exhibited larger An–E vs. Ln–E bond length differences for E = Se and Te than E = S in isomorphous $[M\{N(E{=}PR_2)_2\}_3]$ (R = Ph, *i*Pr) complexes. The largest difference (0.060(4) Å shorter An–E vs. Ln–E) was observed for La^{3+}/U^{3+}, where E = Te and R = *i*Pr.[13d] We hypothesized that if a shorter Am-E vs. Nd-E bond was to be crystallographically observable, the probability would be highest using the heavier Se or Te chalcogen donors. To keep the reaction scale under 5 mg (due to ^{243}Am availability and radiological hazards) we opted for the highly crystalline R = Ph variant, rather than R = *i*Pr. The E = Te variant is not known to be stable for R = Ph so we used LSe, which has also been shown to exhibit significant An–E vs. Ln–E differences within the Pu^{3+}/Ce^{3+} pair.[13d,15] Moreover, there are a limited number of structurally characterized molecular Am complexes,[16] and LSe offered an opportunity to explore a new donor type in molecular Am chemistry. To provide an anticipated purely ionic comparison we then turned to LO ($LO = \{N(O{=}PPh_2)_2\}^{1-}$) as an O-donor analogue of LSe. $[M(LO)_3]$ (M = Ln) complexes are generally 6-coordinate where the N-atom remains unbound,[17] whereas $[M(LSe)_3]$ (M = Ln, An) complexes are 9-coordinate,[13a,d] with intra-ligand steric repulsion previously invoked to rationalize these differences.[13a,d]

Complexes **1-Am** and **2-Am** (Scheme 1) were synthesized by first converting aqueous acidic $^{243}Am^{3+}$ (3.5 mg) into "$AmCl_3(DME)_n$".[12d] For **1-Am** this was used to prepare "$Am(N'')_3$" ($N'' = \{N(SiMe_3)_2\}$) in situ, then layered with a solution of HLSe, which subsequently formed crystals in fair (43 %) yield (Figure 1, left). **1-M** complexes have fairly low solubility even in THF, thus we used a protonolysis layering protocol rather than salt-metathesis using KLSe to avoid troublesome separation of **1-Am** from KCl. Complex **2-Am** was synthesized in water from KLO[18] and "$AmCl_3(DME)_n$", prepared under anhydrous conditions. The precipitated hydrophobic **2-Am** was recrystallized in low (26 %) yield (Figure 1, right). Whilst a simplified protocol using dried

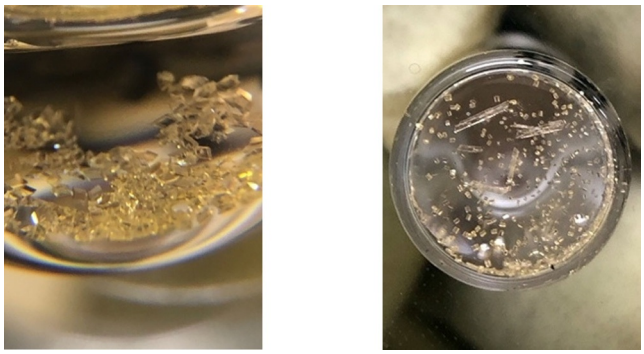

Figure 1. Photographs of the crystals of **1-Am** (left) and **2-Am** (right). While **1-Am** crystallized uniformly as pale-yellow parallelepipeds, **2-Am** formed two different polymorphs.

"$Am^{3+}{}_{(aq)}$" residue with KLO was desirable, this was not successful using Nd^{3+} and neither were attempts using "$NdCl_3(DME)_n$" prepared from dried acidic residue and Me_3SiCl/ DME in air. Therefore, we opted to use the proven route to "$AmCl_3(DME)_n$" performed under inert atmosphere conditions. Both **2-M** (M = Am, Nd) crystallized in multiple different crystal systems which could be identified by morphology (blocks, plates, or rods). Isolated crystals of both **1-M** complexes coated in oil are stable to traces of atmospheric air for several hours with no visible signs of degradation, and solutions in $[D]_8$-THF decolorize slowly over the course of tens of minutes after exposure to air.

1-Nd and **2-Nd** and were prepared similarly (see Supporting Information). The ionic radius of Nd^{3+} (6-coord. 0.983 Å; 8-coord. 1.109 Å) is similar to Am^{3+} (6-coord. 0.975 Å; 8-coord. 1.09 Å) and thus it was chosen as the Ln analogue for structural comparisons.[19] Attempts to synthesize **1-Eu** for spectroscopic comparison to **1-Am** (both M^{3+} ions are f^6) were unsuccessful, with the Eu^{2+} complex $[Eu(LSe)_2(THF)_2]$ (**3**) as the only isolable product.[20] Such a result was not wholly unexpected given the "Eu^{2+}-like" electronic structure of computationally modeled **1-Eu** by Kaltsoyannis.[13c]

The structures of both **1-M** and **2-M** (M = Am, Nd) were determined by single crystal X-ray diffraction (Figure 2 and Figures S16–20) and verified by collection of full data sets from two different crystals for each Am structure. The two data sets feature statistically indistinguishable Am–Se bond lengths (3.0625-

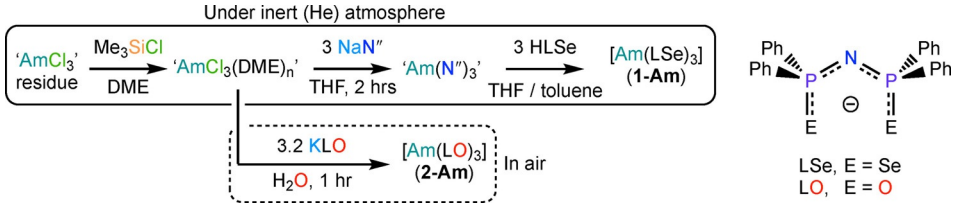

Scheme 1. Synthesis of **1-Am** and **2-Am** (see the Supporting Information). $N'' = \{N(SiMe_3)_2\}^{1-}$, $LSe = \{N(Se{=}PPh_2)_2\}^{1-}$, $LO = \{N(O{=}PPh_2)_2\}^{1-}$.

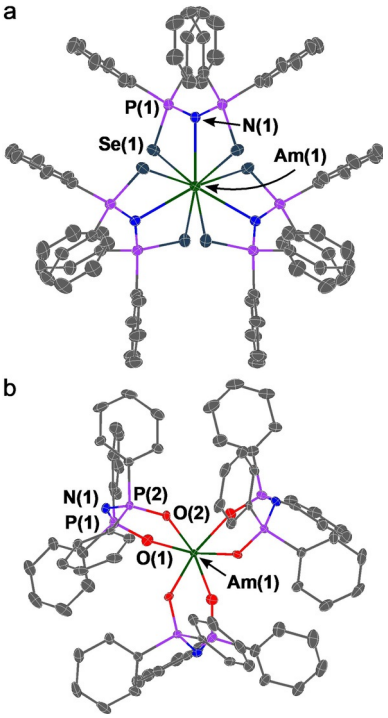

Figure 2. Molecular structures of a) **1-Am** and b) the Am1 molecule of **2-Am**.[36] Ellipsoids set at 50% probability. H-atoms and lattice solvents removed for clarity. a) Am1–Se1 3.0625(8) Å, Am1–N1 2.672(2) Å; P1-N1-P1 144.27(18)°; b) Am1–O1 2.317(3) Å, Am1–O2 2.342(3) Å; P1-N1-P1 128.9(3)°.

(8) and 3.0615(9) Å), the longer of which is used for the following discussion (to guard against over-interpretation) as this represents the smallest difference between **1-Am** and **1-Nd**. Complex **1-Am** crystallized in the centrosymmetric space group $R\bar{3}c$, and is isomorphous with the reported U, Pu, La, Ce congeners, thus comprising a directly comparable series. The Am center is 9-coordinate with all three LSe ligands bound κ^3-*Se,N,Se* and best described as tri-capped trigonal prismatic.[21] A comparison of the M–Se distances in **1-Am** (3.0625(8) Å) and **1-Nd** (3.0801(3) Å) reveals that the Am–Se bond is shorter than the Nd–Se bond (Δ = 0.0176(9) Å) in a statistically meaningful manner (3σ criterion),[22] a noteworthy feature because often Am–L vs. Nd–L distances are statistically indistinguishable from each other. While this is larger than the difference between 6-coord. Nd^{3+}/Am^{3+} (Δ = 0.008 Å), it is smaller than the difference in their 8-coordinate radii (Δ = 0.019 Å, see Supporting Information for more discussion). Thus, we see no structural evidence of increased covalency in this Am^{3+} complex compared to the Nd^{3+} analogue. The difference in M–Se bond lengths was larger for both the U^{3+}/La^{3+} pair (Δ = 0.0360(5) Å) and the Pu^{3+}/Ce^{3+} pair (Δ = 0.0303(4) Å). Therefore, it can be suggested that while the magnitude of the An–Se vs. Ln–Se shortening is statistically equivalent upon moving from U to Pu, there is a significant drop in this difference upon moving to Am, consistent with the traditional view of a transition to more "lanthanide-like" behavior from Pu to Am.[1b,23]

As structures of **1-M** have now been experimentally determined where M = La, Ce, Nd, U, Pu, Am, their M–Se distances can be subjected to more detailed analysis by plotting vs. metal ionic radius (Figure S26).[13a,d] While 8- and 9-coordinate radii are not reported by Shannon for U^{3+}/Pu^{3+}, these values are known for Ln^{3+} ions and Am^{3+}.[19] Coincidentally a straight line of 8-coordinate radius vs. M–Se distance for **1-Ln** (Ln = La, Ce, Nd) passes through our value for **1-Am** when the experimentally determined 8-coordinate radius of Am^{3+} is also used. The M–N distances (**1-Am**, 2.672(2) Å; **1-Nd**, 2.678(3) Å; Δ = 0.006(4) Å) show a significantly smaller An vs. Ln difference than the M–Se bonds. This is not unexpected for softer Se donors with a better energy match to the contracted 5f orbitals as compared to the harder N donors (Table 1).[5,9c,12b,c] Computational work by Kaltsoyannis has highlighted the minor role that the N-atom plays in bonding for these and related complexes.[13c] The Am–Se bond length in **1-Am** is also the longest measured Am-E bond in a molecular system. The closest other examples come from the Am-S bonds in $[n\mathrm{Bu_4N}][\mathrm{Am}\{\mathrm{S_2P}(t\mathrm{Bu_2C_{12}H_6})\}_4]$, $[\mathrm{AsPh_4}][\mathrm{Am}\{\mathrm{S_2P(OEt)_2}\}_4]$ and $[\mathrm{Am}\{\mathrm{S_2C(NEt_2)}\}_3(\mathrm{phen})]$ (phen = 1,10-phenanthroline; range 2.8015(9)–2.969(4) Å across these three),[12c,24] and the Am-Br bonds in $[\mathrm{AmBr_3(THF)_4}]$ and $[\mathrm{AmBr_3(O{=}PCy_3)_3}]$ (range 2.8221(7)–2.9118(13) Å across both).[25]

Table 1: A summary of M–Se and M–N distances in reported f-element **1-M** complexes.

M	M–N [Å]	Δ Ln/An [Å][a]	M–Se [Å]	Δ Ln/An [Å][a]
La	2.706(3)		3.1229(3)	
U	2.701(3)	0.005(4)	3.0869(4)	0.0360(5)
Ce	2.691(3)		3.1013(3)	
Pu	2.668(2)	0.023(4)	3.0710(2)	0.0303(4)
Nd	2.678(3)		3.0801(3)	
Am	2.672(2)	0.006(4)	3.0625(8)	0.0176(9)

[a] Numerical difference, error calculated as the root sum of the squares.

Complex **2-Am** crystallized as two polymorphs ($R\bar{3}$, **2-Am$^{\alpha}$**; $P\bar{3}$, **2-Am$^{\beta}$**); for brevity only **2-Am$^{\alpha}$** is discussed here (see Supporting Information for discussion on both). The two Am centers in the asymmetric unit of **2-Am$^{\alpha}$** are 6-coordinate with three LO ligands bound κ-*O,O*. Each has a distinct geometry with Am1 best described as octahedral, and Am2 is almost perfectly trigonal prismatic.[21,26] The presence of both geometries in the asymmetric unit has been seen previously with f-element imidodiphosphinate complexes.[17b,18,27] The same polymorphs (plus two additional ones) were found for **2-Nd** and were selectively grown via appropriate crystallization conditions. The unique Am–O bonds in **2-Am$^{\alpha}$** (Am1: 2.317(3) and 2.342(3) Å; Am2: 2.342(3) and 2.355(3) Å) are broadly the same between the two geometries, and are mostly indistinguishable from Nd–O bonds in **2-Nd$^{\alpha}$** (Nd1: 2.313(3) and 2.339(3) Å; Nd2: 2.341(3) and 2.340(2) Å).

Prior calculations on a model R = H complex, $[\mathrm{Am}\{\mathrm{N(O{=}PH_2)_2}\}_3]$, predicted an Am–O length of 2.358 Å,[13c] which is slightly larger than those in **2-Am$^{\alpha}$**, however there are no other 6-coordinate An^{3+} analogues using this ligand set to determine trends. Previous work has computationally determined M–Se distances for a number of **1-M** analogues.[13c] We found the Am–Se distance in **1-Am** to be slightly shorter

(3.0625(8) Å) than the calculated value (3.089 Å using a full R = Ph model) which is also longer than the value for Nd–Se in **1-Nd** (3.0801(3) Å). Equivalent computational data is not available to compare with **1-Nd**. That the experimental bond length in **1-Am** is shorter than calculated is not necessarily a sign that calculations underestimated the degree of covalency in the Am–Se bond which is likely small; rather, it is likely that the calculations overestimated the degree of charge transfer which would result in longer bond lengths (see below).[13c] Plots of theoretical M–E (M = U, Np, Pu, Am, Cm; E = O, Te) normalized to U as a zero-point showed that when O donors were investigated the M–E length decreased across the 5f row as ionic radius decreases.[13c] In opposition to this, when the donor was Te instead, the M–Te lengths increased gradually to reach a maximum at Am before a sharp drop at Cm. One way of interpreting this is to consider that the U–Te bond has a much larger covalent contribution than that of an Am-Te bond and is thus much shorter than it would be if purely ionic.[28] Simultaneously, calculations predict larger deviation from formal f orbital population at the Am^{3+} center than that of U^{3+} in model 6-coordinate [M{N(Se=PH_2)$_2$}$_3$] and that a similar observation is seen for Eu^{3+} in the Ln series.[13c] Therefore, in the presence of these soft donors, formal Eu^{3+}/Am^{3+} metal ions appear to behave "M^{2+}-like", resulting in bond lengthening.[13c] This also correlates with our inability to synthesize **1-Eu**, and isolation of the Eu^{2+} complex, **3**, instead. Previous Am studies with S-donor ligands have also yielded Am–S/Nd–S bond length comparisons that do not conclusively reflect covalency differences. For [nBu$_4$N][M{S_2P(tBu$_2$$C_{12}$$H_6$)}$_4$] (M = Am, Nd) the average Am–S and Nd–S distances were 2.921(9) and 2.941(8) Å, respectively; within the 3σ criterion, as is the case for [$AsPh_4$][M{S_2P(OEt)$_2$}$_4$] (M = Am, Nd).[24] Increases in Am^{3+} vs. Nd^{3+} covalency within the [M{N(E = PR_2)$_2$}$_3$] series of molecules, even with soft Se donors, are not conclusive based on bond length differences alone when taking into account the 0.019 Å difference between the 8-coordinate ionic radii of Am^{3+}/Nd^{3+}. Thus, we turned to computational and spectroscopic techniques to probe electronic structure differences.

To allow comparison with previous studies we utilized the GGA PBE functional to compute the orbital compositions of the ground states of **1-M** and **2-M**.[13c,d] We found significant differences in the electronic structure between **1-Am** and **1-Nd** when considering the mixing between the metal f and Se p orbitals. Furthermore, there are substantial differences between the orbital compositions of **1-Am** and **2-Am**. On the other hand, no significant differences were found in the electronic structure of **1-Nd** vs. **2-Nd**. Figure 3 shows the highest occupied molecular orbital (HOMO) for both **1-Am** and **1-Nd**. This MO is principally comprised of metal 5f/4f character (75.43 % for **1-Am**; 91.14 % for **1-Nd**), but in **1-Am** the HOMO has a significant contribution from Se p orbitals that is absent in **1-Nd**. Table 2 compares the relative populations of the f orbitals for **1-M** (M = Am, Nd) and **2-M** (M = Am, Nd). In both **2-Am** and **2-Nd** the frontier f orbitals show almost no mixing with O p orbitals (see Supporting Information Figures S56, S57, and Tables S23, S24), though O-participation is greater in **2-Am** than **2-Nd**. This agrees with previous work which showed that heavier chalcogenide donors resulted in larger metal d participation with ligand bonding orbitals, but that Ln/An differences are mostly in the f orbitals.[13c,d] For **1-M** (M = Am, Nd) the largest metal d contribution to the bonding orbitals is around 9.6 %, while for both **2-M** complexes the metal d contribution is negligible. Varying the metal changes the metal f contribution to bonding orbitals, while varying the chalcogenide changes the metal d contribution.

Table 3 compares the average atomic spin density for all molecules herein. Both **2-M** (M = Am, Nd) have the expected

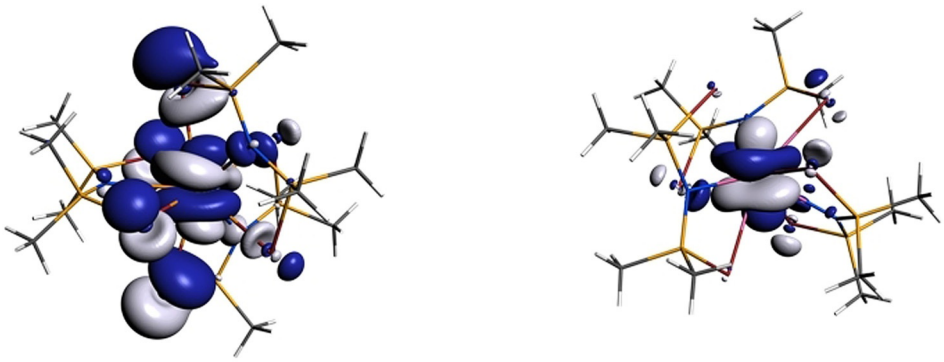

Figure 3. Highest occupied molecular orbitals (HOMOs) of **1-Am** (left) and **1-Nd** (right) (contour value 0.02 a.u.). For **1-Am** there is significant mixing between the metal f and Se p orbitals, which is mostly absent in the **1-Nd** analogue. The entire f manifold for all molecules, as well as select ligand-centered orbitals are available in the Supporting Information, Figures S54–S57.

Table 2: Percent atomic orbital compositions of frontier orbitals for **1-M** and **2-M** (M = Am, Nd).[a]

Frontier Orbital	**1-Am**		**2-Am**		**1-Nd**		**2-Nd**	
	5f	Se p	5f	O p	4f	Se p	4f	O p
HOMO	70.82	17.34	87.25	1.18	91.14	0.00	95.80	0.00
LUMO	75.43	13.34	84.74	1.08	97.38	0.00	92.28	0.00

[a] The compositions of all MOs are also included in the Supporting Information (Tables S21–S24; Figures S54–S57 provide visualizations).

Table 3: Average atomic spin density for each species studied from DFT/PBE.

Molecule	Am/Nd	Se/O	N	P
1-Am	6.248	−0.038	−0.011	−0.001
2-Am	6.059	−0.014	0.000	0.004
1-Nd	3.175	−0.024	−0.007	−0.003
2-Nd	3.053	−0.008	0.000	0.000

metal formal spin (i.e. 6.0 for **2-Am** and 3.0 for **2-Nd**). However, the values for **1-M** (M = Am, Nd) deviate modestly indicating extra charge transfer to the metal center which could indicate some covalent interaction. In the absence of large structural effects, the spin density analysis and orbital compositions point to a charge-transfer-like description of the bonding as previously found by Kaltsoyannis.[9d,13c]

The ground state of Am^{3+} ($5f^6$) is predominantly $^7F_0$ which is formally non-magnetic ($j = 0$) which leads to sharp signals in the NMR spectra of **1-Am** and **2-Am**. The ^{1}H NMR spectrum of **1-Am** in $[D]_8$-THF shows three multiplet resonances at 6.94 (t), 7.13 (t) and 7.69 (q) ppm. The $^{31}P\{^1H\}$ NMR spectrum of **1-Am** shows a sharp singlet at 125.60 ppm, (c.f. HLSe at 53.29 ppm). The $^{77}Se\{^1H\}$ NMR spectrum of **1-Am** exhibits a doublet at −98.10 ppm ($^1J_{SeP} = 604.90$ Hz; c.f. HLSe at −189.14 ppm, $^1J_{SeP} = 800.50$ Hz). Complex **2-Am** was studied in $[D]_2$-DCM as **2-M** complexes can coordinate Lewis bases such as THF.[17a] The ^{1}H NMR spectrum of **2-Am** showed three apparent multiplets at 7.11 (dq), 7.25 (t), and 7.63 (dt) ppm, and the $^{31}P\{^1H\}$ NMR spectrum exhibits a single resonance at 70.95 ppm. Both **1-Nd** and **2-Nd** display ^{1}H NMR spectra where the $^4I_{9/2}$ ground state of Nd^{3+} ($4f^3$) leads to small paramagnetic shifts but broadening that obscures the splitting of the aromatic protons (Supporting Information).

Figure 4 shows solution UV-vis-NIR absorption spectra in THF for **1-M** (M = Am, Nd) and toluene for **2-M** (M = Am, Nd), and solid-state spectra for **1-Am** and **2-Am** from single crystals. For Am^{3+} there are two intense characteristic Laporte-forbidden f→f peaks which derive from $^7F_0 \rightarrow {}^7F_6$ and $^7F_0 \rightarrow {}^5L_6$ transitions, respectively.[1a,29] For the Am^{3+} aquo ion these appear at 12407 and 19881 cm^{-1}.[1a] Splitting of the higher energy peak is not always observed, but was reported for $[Am(Cp^{tet})_3]$, and was reproduced by SO-CASSCF/NEVPT2 calculations; the splitting was rationalized by increased splitting of excited crystal field states.[12d] Other Am^{3+} complexes that show comparable peak splitting have O-donor ligands such as: poly-borate anions for example, $\{B_9O_{13}(OH)_4\}$,[30] or neutral O-donor ligands for example, O=PCy_3.[25b,31] It is likely that this splitting derives not just from ligand field effects, but also solution/solid phase symmetry differences and vibronic coupling.[29,32] This peak can therefore afford insight into fine electronic structure properties.[12b,d]

The experimental UV-vis-NIR spectra suggest differences in electronic structure between the soft donor complexes **1-M** and the harder **2-M** analogues (M = Am, Nd), and highlight Am vs. Nd differences. The solution phase spectrum of **1-Am** (Figure 4a, black line) is dominated by a broad featureless ligand to metal charge transfer (LMCT) band above 26000 cm^{-1}, which appears resolved in the solid-state spectrum into peaks at 26214, 27269, 27950, and 28197 cm^{-1} (Figure 4a, red line). Below this band, the solution spectrum shows two peaks (12050 and 12478 cm^{-1}) that could correspond to the $^7F_0 \rightarrow {}^7F_6$ transition which, due to their proximity, appear in the solid-state spectrum as a broad feature around 12204 cm^{-1}. In the solution spectrum of **2-Am** (Figure 4b, black line) this region appears as three resolved peaks at 12189, 12346 and 12974 cm^{-1}; once again the solid-state spectrum (Figure 4b, red line) is broader with only two resolved peaks (12326 and 12537 cm^{-1}). For the higher energy $^7F_0 \rightarrow {}^7F_6$ transition, neither the solid-state or solution spectrum of **1-Am** shows splitting of the 19448 cm^{-1} peak; but, for **2-Am** in solution this feature appears as four well-resolved peaks (19026, 19531, 19677 and 19778 cm^{-1}) which in the solid-state are less resolved and present as two slightly broad peaks at 19013 and 19661 cm^{-1}. Table 4 shows these data along with that for AmX_3 (X = Cl, Br, and I) and the Am^{3+} aquo ion.[29,32]

In **1-Am** the transition to the $^7F_6$ state shows a notable nephelauxetic shift compared to **2-Am**, similar in size to the differences between $AmCl_3$ and $AmBr_3$.[29b,33] This suggests decreased electron-electron repulsion in the f orbitals of **1-**

Table 4: Selected peaks from the spectra of **1-Am**, **2-Am**, AmX_3 (X = Cl, Br, I), and the Am^{3+} aquo ion in frozen solution.[29,32]

	1-Am	**2-Am**[a]	$AmCl_3$	$AmBr_3$	AmI_3	$Am^{3+}_{(aq)}$
$^7F_6$	12204	12326; 12537	12376	12285	11930	12407
$^5L_6$	19448	19013; 19661	19627	19500	19250	19881

[a] The sets of two peaks for **2-Am** have been assigned by proximity to the known transition, but potentially arise from a different *jj* transition.

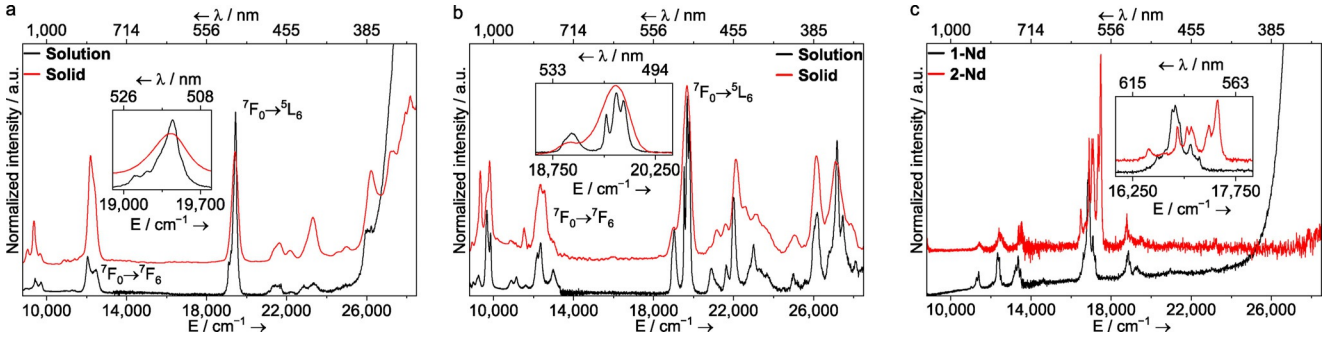

Figure 4. Normalized solution (black line) and solid-state (red line) UV-vis-NIR spectra for a) **1-Am** and b) **2-Am**; and c) solution UV-vis-NIR spectra for **1-Nd** (black line) and **2-Nd** (red line). Spectra truncated to 8800–28500 cm^{-1} (1136–351 nm) and normalized to compare the f→f transitions between the LSe and LO complexes.

Am than **2-Am**, and potentially greater covalent interaction. The same general trend in energy shift also appears to be present for transitions to the $^5L_6$ level, although the 19013 cm^{-1} feature of **2-Am** (this transition is split into multiple peaks for **2-Am**) is an outlier to this trend. When this concept is applied to the peaks of **1-Nd** (Figure 4c, black line), **2-Nd** (Figure 4c, red line), $NdCl_3$, and the Nd^{3+} aquo ion (Table 5) we find that not only is there a very small difference between the spectra of highly ionic **2-Nd**, $NdCl_3$, and the aquo ion, but that **1-Nd** is also essentially the same as these species. This suggests that all of these Nd^{3+} compounds/ions are approximately as ionic as each other. The exception to this is the hypersensitive $^4I_{9/2}\rightarrow{}^4G_{5/2}$ transition which is strongly influenced by local differences in polarizability.

Table 5: Selected peaks from the spectra of **1-Nd**, **2-Nd**, $NdCl_3$, and the Nd^{3+} aquo ion in frozen solution.[34]

	1-Nd	**2-Nd**	$NdCl_3$	$Nd^{3+}_{(aq)}$
$^4F_{3/2}$	11289; 11390	11429	11438	11460
$^4F_{5/2}$	12333 12429	12398	12466	12480
$^4F_{7/2}$, $^4S_{3/2}$	13245; 13351; 13492	13528	13437	13500
$^2K_{13/2}$, $^4G_{7/2}$	18868	18783	18939	19160

The UV-vis-NIR spectra were simulated using the complete active-space self-consistent field theory (CASSCF) including correlation effects via second-order perturbation theory and spin-orbit coupling effects (SO-CASPT2).[35] The complexes were modelled by replacing Ph groups with Me groups (Supporting Information). Simulated spectra for **1-Am** and **2-Am** are shown in Figures 5a and b, respectively (red lines, see Supporting Information for discussion on **1-Nd** and **2-Nd**). For **1-Am** we utilized an active space that included the Am f electrons and orbitals; for **2-Am** we included two occupied ligand orbitals, along with the Am 7s and one Am 6d orbital. We searched for an active space with an Am 6d orbital for **1-Am**, but were unable to find a reasonable solution. We find good agreement in the low energy (9000–15000 cm^{-1}) region, which correspond to f→f transitions that maintain the spin-polarization of the ground state ($S=7$ to $S=7$ transitions). The large peaks at ca. 19500 cm^{-1} in the experimental spectra also appear in the simulations and involve a spin-flip and change in the spin-symmetry of the system ($S=7$ to $S=5$). The energy mismatch between experimental and simulated peaks in the 19500 cm^{-1} region for **1-Am** (Figure 5a), has been observed in other Am^{3+} simulated spectra and likely derives from residual electron correlation effects not fully captured in computationally affordable basis sets of active spaces.[12d] For **2-Am**, the simulation accurately describes the energy of the characteristic ca. 19500 cm^{-1} peak using a larger active space (Figure 5b). However, we were unable to find a larger active space that resulted in a comparable improvement for **1-Am**. While the larger active space used with **2-Am** includes a metal d and s orbital, the observed transitions are almost exclusively LMCT states centered on the f orbitals.

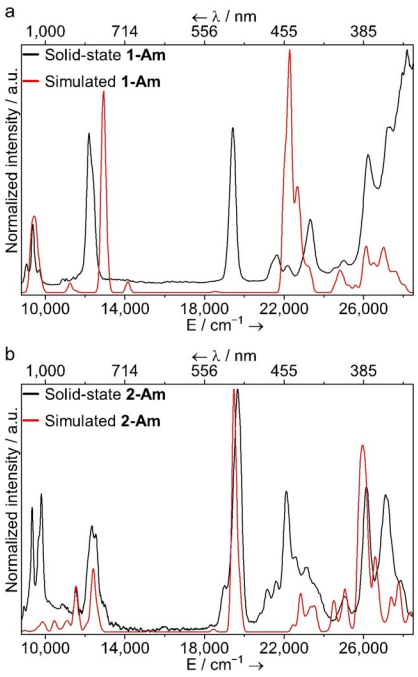

Figure 5. Solid-state experimental (black lines) and SO-CASPT2 simulated (red lines) UV-vis-NIR spectra of a) **1-Am** and b) **2-Am**. The **1-Am** simulation utilized 6 electrons in 7 Am f orbitals, while the **2-Am** simulation utilized 10 electrons in 11 orbitals, which include 7 Am f orbitals, 2 occupied ligand orbitals, plus an Am d and s orbital. No empirical shift has been applied to align the simulated/experimental spectra.

Though the 6d and 7s orbitals are too high in energy for transitions in our experimental range, they play a role in balancing the wavefunction in the perturbation theory treatment. While there are few apparent LMCT states involving the Am d orbital in **2-Am**, we leave the question open whether transitions involving the metal d orbitals are important in the **1-Am** spectrum as we were unable to find a suitable active space that included Am d orbitals. The larger Am d orbital contribution to the bonding orbitals in **1-Am** compared to **2-Am** could result in ligand→d charge transfer states. We observed similar accuracy and features for **1-Nd** and **2-Nd** (Figure S52). We note the simulated spectrum of **2-Am** does not capture the 19013 cm^{-1} shoulder present in the solid-state experimental spectrum.

The experimental UV-vis-NIR spectra suggest a modest degree of increased electron delocalization in the orbitals involved in several key f→f transitions for soft Se-donor **1-Am** over those in hard O-donor **2-Am**; a change absent in both Nd analogues. This is reflected in the MO compositions of all four complexes (Figure 3, Figures S53–S57), which show greater Am 5f participation in bonding MOs for **1-Am** than **2-Am**; again, the Nd complexes are largely the same as each other. Finally, good agreement between simulated and experimental spectra lend credence to this argument that there is a small observed increase in what could be considered covalency in **1-Am** when compared to **1-Nd**, or **2-M** (M = Am, Nd), though all four are still predominantly ionic.

Conclusion

The first molecular transplutonium complex featuring an actinide-Se bond in $[Am\{N(Se{=}PPh_2)_2\}_3]$ (**1-Am**) has been synthesized and compared through structural/spectroscopic analysis to a hard O-donor complex, $[Am\{N(O{=}PPh_2)_2\}_3]$ (**2-Am**), along with their Nd congeners (**1-Nd** and **2-Nd**). Through ab initio and DFT calculations we found that the energetic/spatial proximity of Se 4p orbitals on the soft-donor $\{N(Se{=}PPh_2)_2\}^{1-}$ ligand to the Am 5f manifold resulted in a good degree of mixing and Se composition in the frontier orbitals of **1-Am**. This was not matched in **1-Nd**, which has almost no Se composition in the frontier orbitals. Comparing Am–O/Nd–O bonding with the hard-donor $\{N(O{=}PPh_2)_2\}^{1-}$ ligand, we found that **2-Am** and **2-Nd** were extremely comparable, with little to no O composition in frontier orbitals. Interestingly, the computed electronic structure variations did not manifest as measurable structural differences. However, differences are observed in the UV-vis-NIR spectra of **1-Am** and **2-Am** that may reflect the more diffuse/mixed nature of the occupied molecular orbitals in **1-Am**, whereas the spectrum for **2-Am** is much closer to that of the Am^{3+} aquo ion or $AmCl_3$. Both **1-Nd** and **2-Nd** spectra are largely identical, and comparable to the Nd^{3+} aquo ion or $NdCl_3$. Hence, we observe a greater soft-donor electronic structure effect for Am^{3+} than for Nd^{3+}.

Acknowledgements

We thank the U.S. Department of Energy, Office of Science, Basic Energy Sciences (DOE-BES), Heavy Element Chemistry Program at Los Alamos National Laboratory (LANL) (A.J.G., E.R.B., P.Y., B.L.S., S.A.K., F.D.W.; DE-AC52-06NA25396) for experimental Se donor work and theory, and the Center for Actinide Science and Technology (CAST), an Energy Frontier Research Center (EFRC) funded by DOE-BES for experimental O donor work (A.J.G., T.E.A.S.; DE-SC0016568). C.A.P.G. thanks a distinguished J. R. Oppenheimer Postdoctoral Fellowship (20180703PRD1) and L.M.S. the Exploratory Research program (20190091ER) both under LANL-LDRD (Laboratory Directed Research and Development). A.W.S. thanks a G.T. Seaborg Postdoctoral Fellowship at LANL. During manuscript preparation, we became aware of complementary solution spectroscopic studies on Am^{3+} with the LO ligand by Natrajan and Kaden (S. D. Woodall, Ph.D. Thesis, 2014, The University of Manchester), to be published separately.

Conflict of interest

The authors declare no conflict of interest.

Keywords: actinides · americium · covalency · spectroscopy · structure

[1] a) L. R. Morss, N. M. Edelstein, J. Fuger, *The Chemistry of the Actinide and Transactinide Elements*, Springer, Dordrecht, **2006**; b) J. N. Mathur, M. S. Murali, K. L. Nash, *Solvent Extr. Ion Exch.* **2007**, *19*, 357.

[2] a) B. F. Myasoedov, M. S. Milyukova, E. V. Kuzovkina, D. A. Malikov, N. S. Varezhkina, *J. Less-Common Met.* **1986**, *122*, 195; b) C. J. Dares, A. M. Lapides, B. J. Mincher, T. J. Meyer, *Science* **2015**, *350*, 652; c) K. McCann, D. M. Brigham, S. Morrison, J. C. Braley, *Inorg. Chem.* **2016**, *55*, 11971.

[3] a) L. Karmazin, M. Mazzanti, J. Pécaut, *Chem. Commun.* **2002**, 654; b) D. Girnt, P. W. Roesky, A. Geist, C. M. Ruff, P. J. Panak, M. A. Denecke, *Inorg. Chem.* **2010**, *49*, 9627; c) J. F. Corbey, B. M. Rapko, Z. Wang, B. K. McNamara, R. G. Surbella III, K. L. Pellegrini, J. M. Schwantes, *Inorg. Chem.* **2018**, *57*, 2278; d) G. J. Deblonde, A. Ricano, R. J. Abergel, *Nat. Commun.* **2019**, *10*, 2438; e) T. S. Grimes, C. R. Heathman, S. Jansone-Popova, A. S. Ivanov, V. S. Bryantsev, P. R. Zalupski, *Inorg. Chem.* **2020**, *59*, 138.

[4] A. Bhattacharyya, P. K. Mohapatra, *Radiochem. Acta* **2019**, *107*, 931.

[5] a) M. P. Kelley, J. Su, M. Urban, M. Luckey, E. R. Batista, P. Yang, J. C. Shafer, *J. Am. Chem. Soc.* **2017**, *139*, 9901; b) J. Su, E. R. Batista, K. S. Boland, S. E. Bone, J. A. Bradley, S. K. Cary, D. L. Clark, S. D. Conradson, A. S. Ditter, N. Kaltsoyannis, J. M. Keith, A. Kerridge, S. A. Kozimor, M. W. Loble, R. L. Martin, S. G. Minasian, V. Mocko, H. S. La Pierre, G. T. Seidler, D. K. Shuh, M. P. Wilkerson, L. E. Wolfsberg, P. Yang, *J. Am. Chem. Soc.* **2018**, *140*, 17977.

[6] a) M. Mazzanti, R. Wietzke, J. Pécaut, J. M. Latour, P. Maldivi, M. Remy, *Inorg. Chem.* **2002**, *41*, 2389; b) T. Mehdoui, J. C. Berthet, P. Thuéry, L. Salmon, E. Riviere, M. Ephritikhine, *Chem. Eur. J.* **2005**, *11*, 6994.

[7] a) M. A. Denecke, P. J. Panak, F. Burdet, M. Weigl, A. Geist, R. Klenze, M. Mazzanti, K. Gompper, *C. R. Chim.* **2007**, *10*, 872; b) Z. Kolarik, *Chem. Rev.* **2008**, *108*, 4208.

[8] a) C. Adam, P. Kaden, B. B. Beele, U. Müllich, S. Trumm, A. Geist, P. J. Panak, M. A. Denecke, *Dalton Trans.* **2013**, *42*, 14068; b) C. Adam, B. B. Beele, A. Geist, U. Mullich, P. Kaden, P. J. Panak, *Chem. Sci.* **2015**, *6*, 1548.

[9] a) M. J. Tassell, N. Kaltsoyannis, *Dalton Trans.* **2010**, *39*, 6719; b) I. Kirker, N. Kaltsoyannis, *Dalton Trans.* **2011**, *40*, 124; c) M. L. Neidig, D. L. Clark, R. L. Martin, *Coord. Chem. Rev.* **2013**, *257*, 394; d) N. Kaltsoyannis, *Inorg. Chem.* **2013**, *52*, 3407; e) T. Vitova, I. Pidchenko, D. Fellhauer, P. S. Bagus, Y. Joly, T. Pruessmann, S. Bahl, E. Gonzalez-Robles, J. Rothe, M. Altmaier, M. A. Denecke, H. Geckeis, *Nat. Commun.* **2017**, *8*, 16053.

[10] a) S. T. Liddle, *Angew. Chem. Int. Ed.* **2015**, *54*, 8604; *Angew. Chem.* **2015**, *127*, 8726; b) A. Kerridge, *Chem. Commun.* **2017**, *53*, 6685.

[11] N. Kaltsoyannis, *Chem. Eur. J.* **2018**, *24*, 2815.

[12] a) S. G. Minasian, J. M. Keith, E. R. Batista, K. S. Boland, D. L. Clark, S. D. Conradson, S. A. Kozimor, R. L. Martin, D. E. Schwarz, D. K. Shuh, G. L. Wagner, M. P. Wilkerson, L. E. Wolfsberg, P. Yang, *J. Am. Chem. Soc.* **2012**, *134*, 5586; b) J. N. Cross, J. Su, E. R. Batista, S. K. Cary, W. J. Evans, S. A. Kozimor, V. Mocko, B. L. Scott, B. W. Stein, C. J. Windorff, P. Yang, *J. Am. Chem. Soc.* **2017**, *139*, 8667; c) S. K. Cary, J. Su, S. S. Galley, T. E. Albrecht-Schmitt, E. R. Batista, M. G. Ferrier, S. A. Kozimor, V. Mocko, B. L. Scott, C. E. Van Alstine, F. D. White, P. Yang, *Dalton Trans.* **2018**, *47*, 14452; d) C. A. P. Goodwin, J. Su, T. E. Albrecht-Schmitt, A. V. Blake, E. R. Batista, S. R. Daly, S. Dehnen, W. J. Evans, A. J. Gaunt, S. A. Kozimor, N. Lichtenberger, B. L. Scott, P. Yang, *Angew. Chem. Int. Ed.* **2019**, *58*, 11695; *Angew. Chem.* **2019**, *131*, 11821; e) J. M. Sperling, E. J. Warzecha, C. Celis-Barros, D. C. Sergentu, X. Wang, B. E. Klamm, C. J. Windorff, A. N. Gaiser, F. D. White, D. A. Beery,

A. T. Chemey, M. A. Whitefoot, B. N. Long, K. Hanson, P. Kogerler, M. Speldrich, E. Zurek, J. Autschbach, T. E. Albrecht-Schönzart, *Nature* **2020**, *583*, 396.
[13] a) A. J. Gaunt, B. L. Scott, M. P. Neu, *Chem. Commun.* **2005**, 3215; b) A. J. Gaunt, B. L. Scott, M. P. Neu, *Angew. Chem. Int. Ed.* **2006**, *45*, 1638; *Angew. Chem.* **2006**, *118*, 1668; c) K. I. Ingram, M. J. Tassell, A. J. Gaunt, N. Kaltsoyannis, *Inorg. Chem.* **2008**, *47*, 7824; d) A. J. Gaunt, S. D. Reilly, A. E. Enriquez, B. L. Scott, J. A. Ibers, P. Sekar, K. I. Ingram, N. Kaltsoyannis, M. P. Neu, *Inorg. Chem.* **2008**, *47*, 29.
[14] C. J. Windorff, J. M. Sperling, T. E. Albrecht-Schönzart, Z. Bai, W. J. Evans, A. N. Gaiser, A. J. Gaunt, C. A. P. Goodwin, D. E. Hobart, Z. K. Huffman, D. N. Huh, B. E. Klamm, T. N. Poe, E. Warzecha, *Inorg. Chem.* **2020**, *59*, 13301.
[15] M. B. Jones, A. J. Gaunt, J. C. Gordon, N. Kaltsoyannis, M. P. Neu, B. L. Scott, *Chem. Sci.* **2013**, *4*, 1189.
[16] C. R. Groom, I. J. Bruno, M. P. Lightfoot, S. C. Ward, *Acta Crystallogr. Sect. B* **2016**, *72*, 171.
[17] a) M. A. Katkova, M. E. Burin, A. A. Logunov, V. A. Ilichev, A. N. Konev, G. K. Fukin, M. N. Bochkarev, *Synth. Met.* **2009**, *159*, 1398; b) H. V. Stafford, *PhD. Thesis*, The University of Manchester, **2019**.
[18] S. W. Magennis, S. Parsons, Z. Pikramenou, *Chem. Eur. J.* **2002**, *8*, 5761.
[19] R. D. Shannon, *Acta Crystallogr. Sect. A* **1976**, *32*, 751.
[20] M. Geissinger, J. Magull, *Z. Anorg. Allg. Chem.* **1997**, *623*, 755.
[21] M. Llunell, D. Casanova, J. Cirera, P. Alemany, S. Alvarez, SHAPE 2.1: Program for the Stereochemical Analysis of Molecular Fragments by Means of Continuous Shape Measures and Assosciated Tools, http://www.*ee*.ub.edu, **2013**.
[22] W. Clegg, A. J. Blake, J. M. Cole, J. S. O. Evans, P. Main, S. Parsons, D. J. Watkin, *Crystal Structure Analysis*, Oxford University Press (2nd ed.) **2009**, p. 240.
[23] a) J. H. Burns, J. R. Peterson, J. N. Stevenson, *J. Inorg. Nucl. Chem.* **1975**, *37*, 743; b) M. P. Jensen, A. H. Bond, *J. Am. Chem. Soc.* **2002**, *124*, 9870; c) S. K. Cary, M. Vasiliu, R. E. Baumbach, J. T. Stritzinger, T. D. Green, K. Diefenbach, J. N. Cross, K. L. Knappenberger, G. Liu, M. A. Silver, A. E. DePrince, M. J. Polinski, S. M. Van Cleve, J. H. House, N. Kikugawa, A. Gallagher, A. A. Arico, D. A. Dixon, T. E. Albrecht-Schmitt, *Nat. Commun.* **2015**, *6*, 6827.
[24] a) J. N. Cross, J. A. Macor, J. A. Bertke, M. G. Ferrier, G. S. Girolami, S. A. Kozimor, J. R. Maassen, B. L. Scott, D. K. Shuh, B. W. Stein, S. C. Stieber, *Angew. Chem. Int. Ed.* **2016**, *55*, 12755; *Angew. Chem.* **2016**, *128*, 12947; b) R. D. M. Greer, C. Celis-Barros, J. M. Sperling, A. N. Gaiser, C. J. Windorff, T. E. Albrecht-Schönzart, *Inorg. Chem.* **2020**, *59*, 16291.
[25] a) S. S. Galley, J. M. Sperling, C. J. Windorff, M. Zeller, T. E. Albrecht-Schmitt, S. C. Bart, *Organometallics* **2019**, *38*, 606; b) C. J. Windorff, C. Celis-Barros, J. M. Sperling, N. C. McKinnon, T. E. Albrecht-Schmitt, *Chem. Sci.* **2020**, *11*, 2770.
[26] R. Ketkaew, Y. Tantirungrotechai, P. Harding, G. Chastanet, P. Guionneau, M. Marchivie, D. J. Harding, *Dalton Trans.* **2021**, *50*, 1086.
[27] A. P. Bassett, R. Van Deun, P. Nockemann, P. B. Glover, B. M. Kariuki, K. Van Hecke, L. Van Meervelt, Z. Pikramenou, *Inorg. Chem.* **2005**, *44*, 6140.
[28] M. P. Kelley, I. A. Popov, J. Jung, E. R. Batista, P. Yang, *Nat. Commun.* **2020**, *11*, 1558.
[29] a) W. T. Carnall, B. G. Wybourne, *J. Chem. Phys.* **1964**, *40*, 3428; b) R. G. Pappalardo, W. T. Carnall, P. R. Fields, *J. Chem. Phys.* **1969**, *51*, 1182.
[30] M. J. Polinski, S. Wang, E. V. Alekseev, W. Depmeier, T. E. Albrecht-Schmitt, *Angew. Chem. Int. Ed.* **2011**, *50*, 8891; *Angew. Chem.* **2011**, *123*, 9053.
[31] G. Tian, D. K. Shuh, C. M. Beavers, S. J. Teat, *Dalton Trans.* **2015**, *44*, 18469.
[32] W. T. Carnall, *J. Less-Common Met.* **1989**, *156*, 221.
[33] A. Barbanel', *Radiochim. Acta* **1997**, *78*, 91.
[34] W. T. Carnall, P. R. Fields, K. Rajnak, *J. Chem. Phys.* **1968**, *49*, 4424.
[35] a) B. O. Roos, P. R. Taylor, P. E. M. Sigbahn, *Chem. Phys.* **1980**, *48*, 157; b) P.-Å. Malmqvist, B. O. Roos, *Chem. Phys. Lett.* **1989**, *155*, 189; c) C. Angeli, R. Cimiraglia, S. Evangelisti, T. Leininger, J. P. Malrieu, *J. Chem. Phys.* **2001**, *114*, 10252; d) C. Angeli, R. Cimiraglia, J.-P. Malrieu, *Chem. Phys. Lett.* **2001**, *350*, 297; e) C. Angeli, R. Cimiraglia, J.-P. Malrieu, *J. Chem. Phys.* **2002**, *117*, 9138; f) F. Neese, *J. Chem. Phys.* **2005**, *122*, 034107; g) F. Neese, *WIRES Comput. Mol. Sci.* **2018**, *8*, e1327.
[36] Deposition Numbers 2020987, 2020988, 2020989, 2020990, 2020991, 2020992, 2020993, 2020994, 2020995, 2020996, 2020997, and 2020998 contain the supplementary crystallographic data for this paper. These data are provided free of charge by the joint Cambridge Crystallographic Data Centre and Fachinformationszentrum Karlsruhe Access Structures service www.ccdc.cam.ac.uk/structures.